Proceedings of the Twenty-eighth (2018) International Ocean and Polar Engineering Conference
Sapporo, Japan, June 10-15, 2018

ISBN 978-1-880653-87-6; ISSN 1098-6189

www.isope.org

Numerical Study on Run-up and Wave Impacts between Breaking Wave and a Circular Cylinder

Zhenghao Liu, Decheng Wan, Gang Chen*

Key Laboratory of Ocean Engineering, School of Naval Architecture, Ocean and Civil Engineering, Shanghai Jiao Tong University, Collaborative Innovation Center for Advanced Ship and Deep-Sea Exploration, Shanghai, China
*Corresponding author

ABSTRACT

Accurate prediction of hydrodynamic loads on offshore structures is of great importance for the safety design of offshore platforms in severe environment. In this work, the generation of breaking focusing wave is carried out and the wave loads on a truncated circular cylinder is investigated using the in-house CFD solver naoe-FOAM-SJTU. The time history of wave elevation at focusing location is compared with experimental data provided by KRISO. The numerical forces, pressures and the scattered wave surface elevations around the cylinder are presented. The results show that the present CFD solver can be an effective tool to deal with breaking wave-structure interactions.

KEY WORDS: Wave-structure interactions; breaking wave; wave force; naoe-FOAM-SJTU solver

INTRODUCTION

Wave breaking is one of the most common sea conditions and plays an important role in many engineering problems. The forces from breaking waves have been a major concern in coastal and offshore engineering. Evaluation of breaking wave impact on fixed or floating structures is of great significance. Theoretical approaches for studying breaking wave forces are generally based on the Morison formula (Morison et al., 1950). Due to the high impact forces during a breaking wave process, an impact force term must be added to Morison formula to describe the total force from breaking waves. However, theoretical approaches are still inadequate in evaluating wave breaking force. So numerous researchers have done experimental and numerical studies on breaking wave forces on cylinders.

Previous investigations of wave forces on cylinders were mainly carried out by model tests performed in a marine basin. Wienke and Oumeraci (2005) examined the plunging breaking waves acting on a slender cylindrical pile. The time history and the intensity of slamming force were analyzed. They found that the impact force was strongly depended on the distance between breaking location and cylinder. Zang et al. (2010) carried out physical experiments on the interaction of breaking and nonbreaking steep waves with a fixed vertical cylinder. The free surface deformation around the cylinder and the horizontal forces for different wave conditions were investigated. Arntsen et al. (2011) conducted small scale experimental tests and presented the results of plunging breaking wave impact forces on a single fixed vertical cylinder. They found that the slamming force intensity along a vertical pile is triangularly distributed. Mo et al. (2013) performed laboratory experiments for solitary waves breaking on a constant slope and investigated the impact of a shoaling solitary wave on a vertical cylinder. Kim and Kim (2001) used the diffraction and the Morison method with a universal nonlinear input output model to simulate the impact forces and wave kinematics of a Draupner freak wave on a vertical cylinder.

In recent years, numerical simulation methods based on Computational Fluid Dynamics (CFD) have been playing a more and more significant role in studying the wave breaking process and the hydrodynamic forces due to the breaking waves, because it can provide detailed description of the physical processes. Bredmose and Jacobsen (2010) investigated breaking wave loads on a monopile and discussed the focus location of wave group on the wave forces using Navier-Stokes equations with the volume of fluid (VOF) method. Choi et al. (2015) studied breaking wave impact forces on a vertical cylinder and inclined cylinders. To remove the effect of dynamic amplification in the experimental data, they employed a low pass filter and EMD (Empirical Mode Decomposition), and the filtered results agree well with the numerical results. Kamath et al. (2015, 2016) used the open source CFD model REEF3D (Bihs et al., 2016) to simulate periodic breaking wave forces on a slender cylinder in a three-dimensional wave tank. The breaking wave impacts the cylinder at different stages of wave breaking and the resulting wave forces were evaluated. Chella et al. (2016) investigated the interaction of plunging breaking waves with a vertical slender cylinder in shallow waters both experimentally and numerically. The numerical model is based on the incompressible Reynolds-averaged Navier-Stokes equations (RANS) with the k-ω for turbulence and the level set method for free surface. Good agreement can be acquired between the numerical results and the experimental data. Bihs et al. (2017) investigated focused wave generation, kinematics, and the interaction with a vertical circular cylinder with the CFD solver REEF3D. Chen et al. (2014) numerically investigated the interaction of focusing waves with a vertical circular cylinder using OpenFOAM. Jose et al. (2017) applied two different 3D Navier-Stokes solvers, 2PM3D (FDM) and OpenFOAM (FVM) to simulate the breaking wave forces on a monopile structure, and found the breaking

wave interaction with the monopile were in good agreement with experimental data for both models.

The objective of the present work is to investigate the breaking wave force on a vertical circular cylinder which is part of comparative study on breaking wave impact loads on a circular cylinder. In this paper, present CFD calculations are performed by the in-house CFD solver naoe-FOAM-SJTU. The time history of focusing wave at target location was compared with the experimental data provided by Korea Research Institute of Ships and Ocean Engineering (KRISO). The results show that the current approach can be an alternative tool to generate breaking waves according to experiment. The local wave forces at six locations and pressures at five locations on the vertical circular cylinder were presented. Details of the breaking wave properties around the cylinder are also given.

The paper is organized as follows: next section presents the numerical methods including governing equations, Volume of fluid (VOF) method, numerical wave tank and discretization schemes; after that we describe the details of experimental setup and numerical model; In the next part, the validation of breaking focusing wave generation and local wave forces and pressures are given; finally, some conclusions of this work are drawn.

NUMERICAL METHODS

Governing Equations

The CFD solver naoe-FOAM-SJTU is based on the open source platform OpenFOAM and designed for the application in ship and ocean engineering field (Shen et al., 2015; Wang et al., 2015; Wang and Wan, 2016; Wang et al., 2016, Zhao and Wan, 2016).

The naoe-FOAM-SJTU solver uses the incompressible unsteady Reynolds averaged Navier-Stokes (URANS) equations with the continuity equation to solve the fluid flow problem:

$$\nabla \cdot \boldsymbol{U} = 0 \tag{1}$$

$$\frac{\partial \rho \boldsymbol{U}}{\partial t} + \nabla \cdot (\rho(\boldsymbol{U} - \boldsymbol{U}_g)\boldsymbol{U}) = -\nabla p_d - \boldsymbol{g} \cdot x \nabla \rho + \nabla \cdot (\mu_{eff} \nabla \boldsymbol{U}) + (\nabla \boldsymbol{U}) \cdot \nabla \mu_{eff} + f_\sigma + f_s \tag{2}$$

where $\boldsymbol{U}$ and $\boldsymbol{U}_g$ are the velocity field and the velocity of grid nodes, respectively. p_d is the dynamic pressure and p is the total pressure, ρ is the mixed density of the two phases water and air. μ_{eff} is the effective dynamic viscosity, in which ν and ν_t are kinematic viscosity and eddy viscosity, respectively. f_σ is the surface tension, which impacts the free surface. f_s is a source term, added to generate the sponge layer for wave absorbing.

VOF Method

To model the two-phase flow, level set method and volume of fluid (VOF) method are always used in CFD solvers. VOF method (Hirt and Nichols, 1981) with artificial bounded compression techniques is adopted in naoe-FOAM-SJTU solver to capture the free surface. The interface between the two phases is determined by introduction of an advection equation:

$$\frac{\partial \alpha}{\partial t} + \nabla \cdot [(\boldsymbol{U} - \boldsymbol{U}_g)\alpha] + \nabla \cdot [\boldsymbol{U}_r(1-\alpha)\alpha] = 0 \tag{3}$$

where α is the volume fraction. For an interface cell, the value of volume fraction α is between 0 and 1, representing it contains both water and air.

$$\begin{cases} \alpha = 0 & \text{air} \\ \alpha = 1 & \text{water} \\ 0 < \alpha < 1 & \text{interface} \end{cases} \tag{4}$$

In physical domain, the density of fluid ρ and the dynamic viscosity μ can be obtained by a weighted value based on the volume fraction α:

$$\rho = \alpha\rho_1 + (1-\alpha)\rho_2 \tag{5}$$

$$\mu = \alpha\mu_1 + (1-\alpha)\mu_2 \tag{6}$$

Where ρ_1 and $\rho_2$denote the density of water and air, μ_1 and μ_2 denote the viscosity coefficient of water and air, respectively.

Numerical Wave Tank

Three wave making modules including piston-type wave maker, flap-type wave maker and velocity are extended to the in-house naoe-FOAM-SJTU solver. Generally, the velocity inlet (Dirichlet-type boundary conditions) is adopted to generate regular or irregular waves, while the piston-type and flap-type wave maker are used to replicate the wave generation of physical experiments. The displacement of paddle in the experiment can be simulated by a moving boundary and dynamic mesh. The wave absorption is required to avoid the wave reflection from the outlet. In naoe-FOAM-SJTU, two kinds of wave absorption are implemented. One is sponge layer which is setup at the outlet of the computational domain. The other uses the paddles at the outlet to absorb waves (Higuera et al., 2013; 2014a; 2014b, 2015). It monitors the water level at the paddles and corrects the movement of the paddles every timestep. A correct velocity is introduced for the correction:

$$u_{corr} = \frac{\omega}{Hs}(\eta_m - \eta_0) \tag{7}$$

Where η_m, η_0 are the measured level and theory level monitored every timestep

Discretization Schemes

The finite volume method (FVM) is adopted to discretize the RANS and VOF transport equations in OpenFOAM. Van Leer scheme is applied for VOF equation. The merged PISO-SIMPLE algorithm is used to solve the coupled equation of velocity and pressure. The convection terms are solved by a second-order TVD limited linear scheme, and the diffusion terms are approximated by a second-order central difference scheme.

Wave Forces Calculation

Wave forces on a structure are generally calculated by integrating the pressure p and wall shear stress τ over the surface Ω of the structure as given by:

$$F = \int_\Omega (-\mathbf{n}p + \mathbf{n} \cdot \tau) d\Omega \tag{8}$$

where $\mathbf{n}$ is the unit normal vector to the surface and Ω is the surface of the structure.

GEOMETRY AND TEST CONDITIONS

Experimental Setup

Present work is part of the comparative study on breaking wave impact loads on a circular cylinder. The physical experiments were carried out in KRISO wave tank. The wave tank is 31 m long with a 3.8 m wave absorber. The wavemaker uses piston-type paddles to generate two-dimensional focusing wave (wave components propagating in same direction). Three types of focusing wave including steep wave, spilling wave and plunging wave were generated in the experiments. For each case, the water depth was set to 0.5 m. Sampling rate for wave elevation measurement is 200 Hz. The focusing point is 17.8 m from wave maker and the focusing is 38.5 s. Fig. 1 shows the physical wave tank.

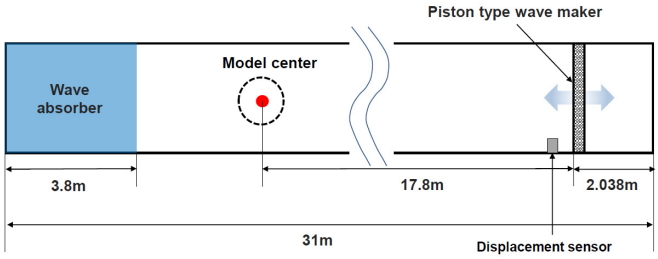

Fig. 1 Physical wave tank

Each wave condition is repeated for five times to prove that the experiments can be reproduced. The paddle displacement signals for five times are shown in Fig. 2. The provided results indicate that the error of wave elevation at focusing location from each experiment can be neglected. A truncated circular cylinder was placed at 17.8 m (focusing location) to evaluate the breaking wave impact. The diameter of the cylinder is 0.25 m, the draft is 0.30 m and the water depth is still 0.50 m. Fig. 3 illustrates the geometry of the physical model and the numerical model. Fig. 4 shows the distribution of 6 local force sensors and 5 pressure sensors.

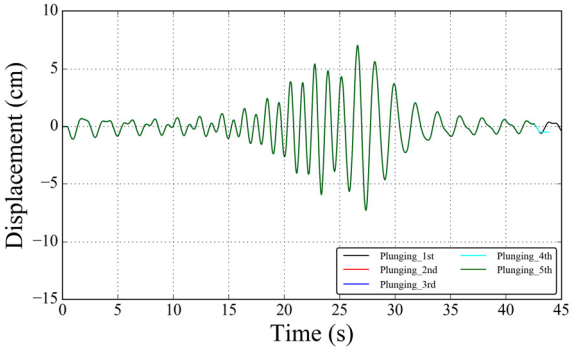

Fig. 2 Displacement of wave generation paddle in physical experiment

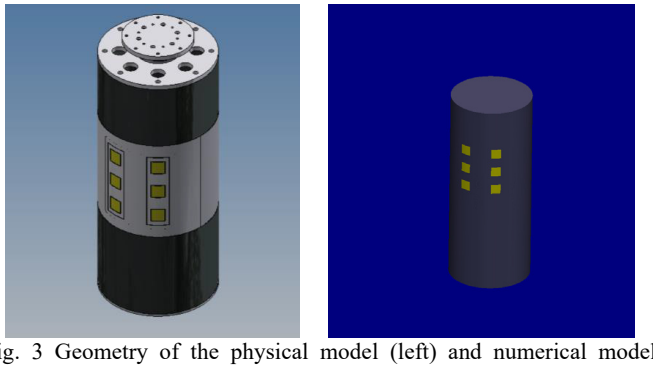

Fig. 3 Geometry of the physical model (left) and numerical model (right)

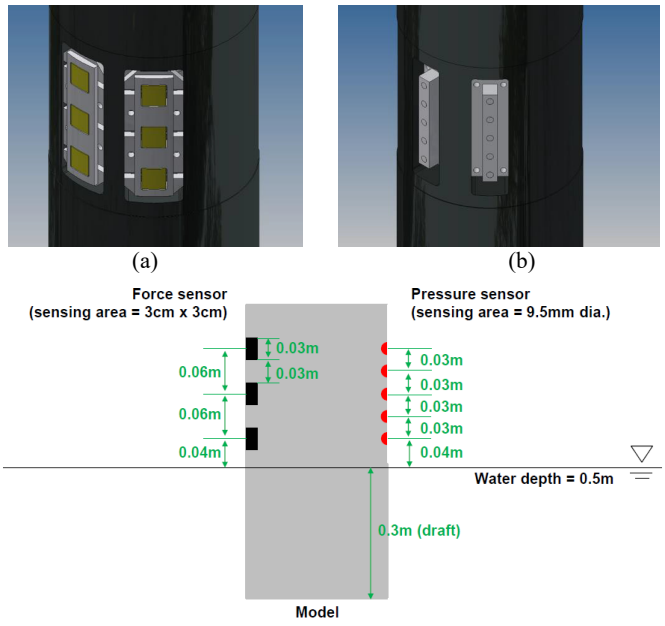

Fig. 4 Distribution of (a) local force sensors, (b) pressure sensors and (c) vertical location of force sensors and pressure sensors.

Numerical Models

Using the CFD solver naoe-FOAM-SJTU, the plunging type focusing wave is simulated without and with the fixed cylinder. According to the physical experiment, the numerical domain was set to $0 < x < 25$ m, -0.5 m $< y < 0.5$ m, -0.5 m $< z < 0.5$ m. The computational mesh is shown in Fig. 5. The total grid number is about 3.5 million for the case without cylinder and 5.5 million for the case with cylinder. Wave generation in the physical wave tank is made with a piston-type wave maker. A series of time and displacement of the wave maker are provided by KRISO which is used as the input signal of the wave generation boundary (moving inlet). The wave generation boundary is located at $x = 0$ m. The vertical cylinder is fixed at $x = 17.8$ away from the inlet. The turbulence was modelled by laminar. Moving-wall inlet boundary condition was adopted to generate the focusing and the wave absorption at the outlet also by moving-wall boundary condition (several paddles). Slip boundary condition was considered at the bottom and at side boundaries. Non-slip boundary condition was set at the cylinder surface. To make it easy to converge in each time step, the interface Courant number was controlled to be under 0.3. The time step is 0.001s in each case.

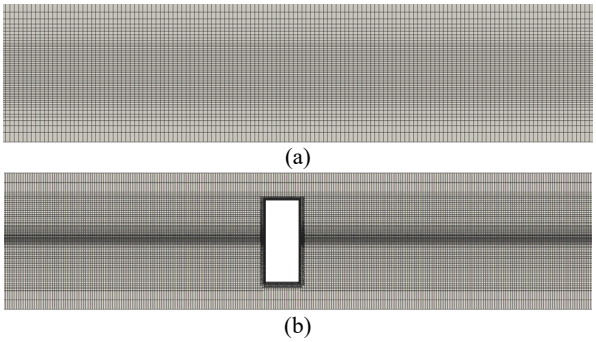

Fig. 5 Computational mesh: (a) without cylinder (b) with cylinder

RESULTS AND DISCUSSION

Validation of Wave Generation

To validate wave generation and propagation in naoe-FOAM-SJTU solver, the numerical results are compared with experimental data provided by KRISO. The time history of free surface elevation at the focusing location (x = 17.8 m) without cylinder is investigated. As shown in Fig. 6, both the phase and the amplitude of numerical free surface elevation are generally consistent with experimental one. The maximum amplitudes of numerical and experimental results are 0.152 m and 0.157 m, respectively. The error between them is -3.1%. It can be found that the amplitude of free surface increases until the focus time and reaches the maximum height at the focus time. A very sharp wave crest and deep wave trough can be found at the focus time. After the focus time, the amplitude of surface elevation decreases, as the energy content of the wave decreases. This indicates that the focusing wave in experiment is well replicated by the wave generated by naoe-FOAM-SJTU solver.

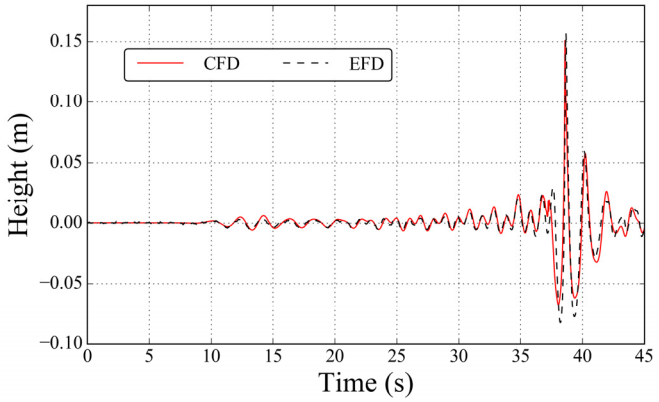

Fig. 6 Comparison of numerical and experimental free surface elevation at x = 17.8 m

Fig. 7 presents the free surface during the breaking process at different time instants. When the focusing wave height increases, the wave becomes asymmetric with the front face being vertical, and a tip forms shown in Fig. 7(a)~(b). Then the tip with high velocity moves forward and evolves into an overturning plunging jet in Fig. 7(c)~(e). When the plunging jet falls on the surface of the preceding wave, a splash-up occurs with the secondary wave crest as shown in Fig. 7(f)~(g). This indicates that the breaking processing are represented well in the present numerical simulation.

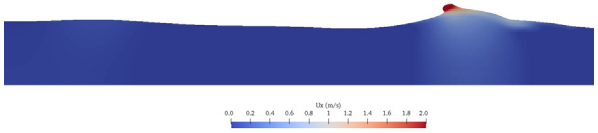

(a)

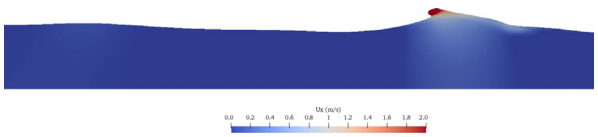

(b)

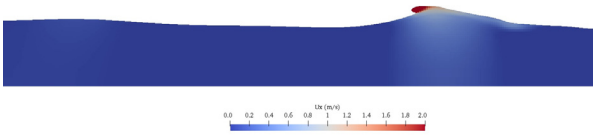

(c)

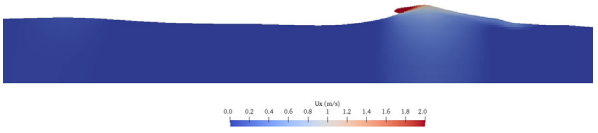

(d)

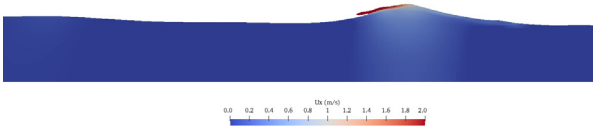

(e)

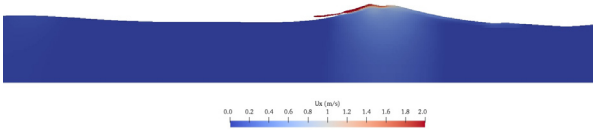

(f)

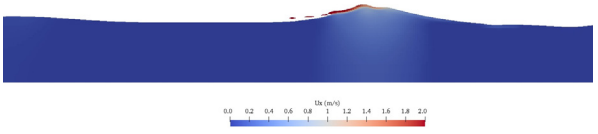

(g)

Fig. 7 Free surface flow features during the breaking process at different time instants

Grid Convergence Study

A grid convergence study has been carried out to validate the accuracy of the current numerical model. Four different meshes by changing grid sizes in z direction with total grid size of 1.3 million (coarse grid), 2.3 million (medium grid), 3.5 million (fine grid) and 8.0 million (finer grid) are compared with experimental data in Fig. 8. The results in Fig. 8 show that the amplitudes of wave at focusing location are 0.114 m, 0.123 m, 0.1520 m and 0.1519 m for coarse grid, medium grid, fine grid and finer grid, respectively. The errors are -27.4%, -21.6%, -3.1% and -3.1%. Neither coarse grid nor medium grid is sufficient to simulate the breaking focusing wave. The comparison of results between the fine grid and finer grid shows that the fine grid is converged numerically. Hence, a fine grid size was chosen for the simulations in the present work.

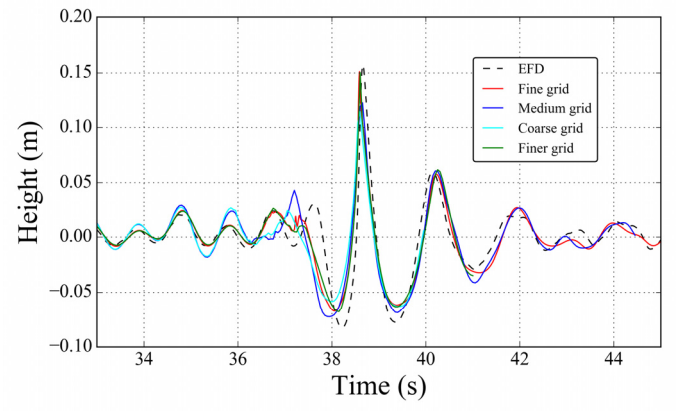

Fig. 8 Free surface elevation at x = 17.8 m for different grid numbers

Breaking Wave Interaction with the Cylinder

The interaction of breaking waves with the cylinder and the resulting breaking wave forces are investigated. Six force sensors are set at the cylinder surface according to experiment as shown in Fig. 4. Five pressure sensors are set to investigate the pressure distribution on the surface during the breaking wave interaction process. Fig. 9 shows the free surface when the focusing wave interacts with the cylinder. When the wave travels towards and impacts the cylinder, strong run-up and nonlinearity in front of the cylinder can be found in Fig. 9(a)~(b). Then the wave propagates further, strong nonlinearity at the rear of the cylinder can be seen as shown in Fig. 9(c)~(d).

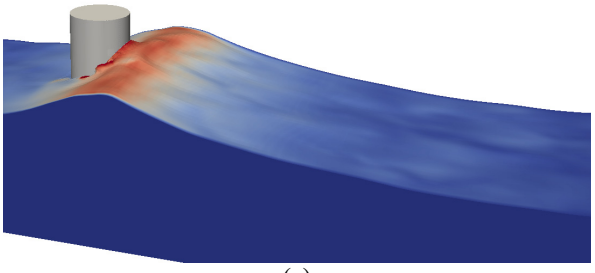

(a)

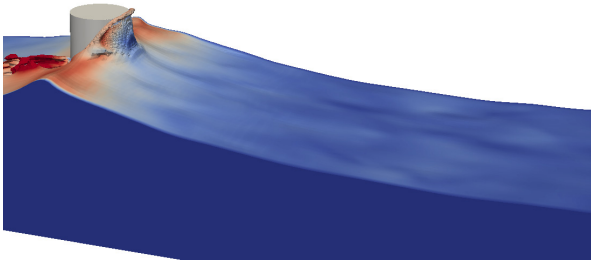

(b)

(c)

(d)

Fig. 9 Free surface elevations during the interaction for different time instants

As shown in Fig. 4(b), 5 pressure sensors at the rear of the cylinder. Fig. 10 shows the pressure time history of the five pressure sensors. P1 is the bottom sensor and P5 is the top pressure sensor in z direction. From P5 to P1, the predicted pressure increases. Fig. 11 shows the local forces at the front of the cylinder.

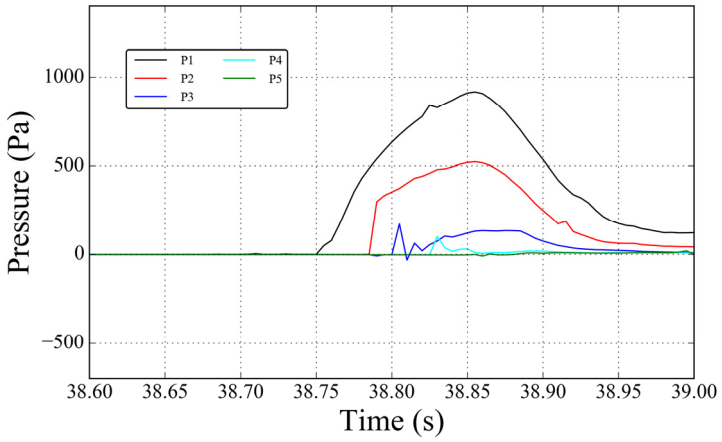

Fig. 10 Predicted pressure time history at the rear of the cylinder

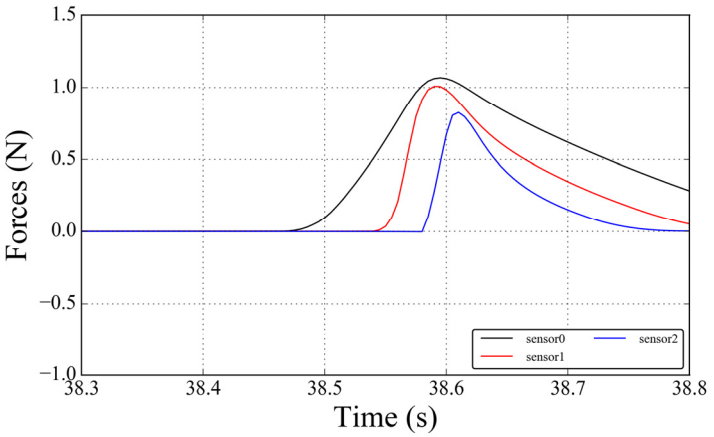

(a)

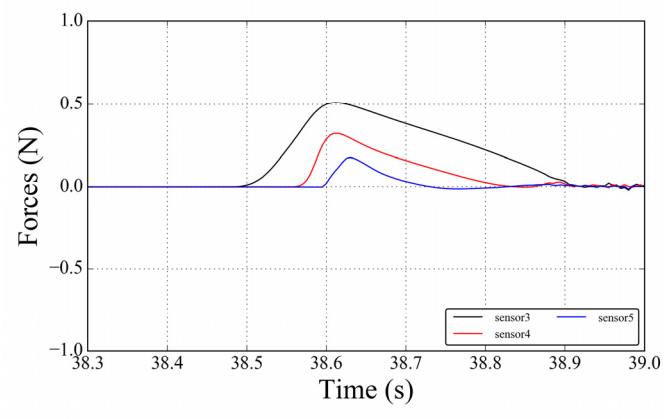

(b)

Fig. 11 Predicted pressure time history at the front of the cylinder: (a) 45 degree with incident wave direction (b) 0 degree with incident wave direction

CONCLUSIONS

The work in this paper is part of comparative study on breaking wave impact loads on a circular cylinder. The numerical generation of breaking focusing wave is carried out using the in-house CFD solver naoe-FOAM-SJTU and the time history of wave elevation at focusing location and focusing time is in good agreement with experimental data provided by KRISO. A grid convergence study has been conducted to validate the accuracy of the current numerical model. Then the interaction between breaking waves and a truncated circular cylinder is investigated. The scattered wave surface elevations around the cylinder are presented. Details of the breaking wave properties around the cylinder are also discussed. Further work on local wave force and pressure distribution will be presented. The results show that the present CFD solver can be an effective tool to deal with breaking wave generation and wave-structure interactions.

ACKNOWLEDGEMENTS

This work is supported by the National Natural Science Foundation of China (51490675, 11432009, 51579145), Chang Jiang Scholars Program (T2014099), Shanghai Excellent Academic Leaders Program (17XD1402300), Program for Professor of Special Appointment (Eastern Scholar) at Shanghai Institutions of Higher Learning (2013022), Innovative Special Project of Numerical Tank of Ministry of Industry and Information Technology of China (2016-23/09) and Lloyd's Register Foundation for doctoral student, to which the authors are most grateful.

REFERENCES

Arntsen, ØA, Ros, X, Tørum, A (2011). "Impact Forces on a Vertical Pile from Plunging Breaking Waves," *Coast Struct*, 2, 533-544.

Bihs, H, Chella, MA, Kamath, A, and Arntsen, ØA (2017). "Numerical Investigation of Focused Waves and Their Interaction With a Vertical Cylinder Using REEF3D," *J Offshore Mech Arct Eng*, 139(4), 041101.

Bihs, H, Kamath, A, Chella, MA, Aggarwal, A, and Arntsen, ØA (2016). "A New Level Set Numerical Wave Tank with Improved Density Interpolation for Complex Wave Hydrodynamics," *Comput Fluids,* 140, 191-208.

Bredmose, H, and Jacobsen, NG (2010). "Breaking Wave Impacts on Offshore Wind Turbine Foundations: Focused Wave Groups and CFD," *Proc 29th Int Conf on Offshore Mech and Arct Eng*, Shanghai, OMAE, 397-404.

Chella, MA, Collados, XR, Bihs, H, Myrhaug, D, and Arntsen, ØA (2016). "Numerical and Experimental Investigation of Breaking Wave Interaction with a Vertical Slender Cylinder," *Energy Procedia*, 94, 443-451.

Chen, LF, Zang, J, Hillis, AJ, Morgan, GCJ, and Plummer, AR (2014). "Numerical Investigation of Wave-Structure Interaction Using OpenFOAM," *Ocean Eng*, 88, 91-109.

Choi, S, Lee, K, and Gudmestad, O (2015). "The Effect of Dynamic Amplification due to a Structures Vibration on Breaking Wave Impact. *Ocean Eng*, 96, 8-20.

Higuera, P, Lara, JL, and Losada, IJ (2013). "Realistic Wave Generation and Active Wave Absorption for Navier-Stokes Models: Application to OpenFOAM," *Coast Eng*, 71, 102-118.

Higuera, P, Lara, JL, and Losada, IJ (2014a). "Three-dimensional Interaction of Waves and Porous Coastal Structures Using OpenFOAM. Part I: Formulation and Validation," *Coast Eng*, 83, 243-258.

Higuera, P, Lara, JL, and Losada, IJ (2014b). "Three-dimensional Interaction of Waves and Porous Coastal Structures Using OpenFOAM. Part II: Application," *Coast Eng*, 83, 259-270.

Higuera, P, Lara, JL, and Losada, IJ (2015). "Three-dimensional Numerical Wave Generation with Moving Boundaries," *Coast Eng*, 101, 35-47.

Hirt, CW, Nichols, BD (1981). "Volume of Fluid (VOF) Method for the Dynamics of Free Boundaries," *J Comput Phys*, 39, 201-225.

Jose, J, Choi, SJ, Giljarhus, KET, and Gudmestad, OT (2017). "A Comparison of Numerical Simulations of Breaking Wave Forces on a Monopile Structure Using Two Different Numerical Models Based on Finite Difference and Finite Volume Methods," *Ocean Eng*, 137, 78-88.

Kamath, A, Chella, MA, Bihs, H, and Arntsen, ØA (2015). "CFD Investigations of Wave Interaction with a Pair of Large Tandem Cylinders," *Ocean Eng*,108, 734-748.

Kamath, A, Chella, MA, Bihs, H, and Arntsen, ØA (2016). "Breaking Wave Interaction with a Vertical Cylinder and the Effect of Breaker Location," *Ocean Eng*, 128, 105-115.

Kim, N, and Kim, CH (2003). "Simulation of Draupner Freak Wave Impact Force on a Vertical Truncated Cylinder," *Int J Offshore and Polar Eng*, ISOPE, 13(04), 260-265.

Mo, W, Jensen, A, and Liu, PLF (2013). "Plunging Solitary Wave and its Interaction with a Slender Cylinder on a Sloping Beach," *Ocean Eng*, 74, 48-60.

Morison, JR, Johnson, JW, and Schaaf, SA (1950). "The Force Exerted by Surface Waves on Piles," *J Petrol Technol*, 2(5), 149-154.

Shen, ZR, Wan, DC, Carrica, PM (2015). "Dynamic Overset Grids in OpenFOAM with Application to KCS Self-propulsion and Maneuvering," *Ocean Eng*, 108, 287-306.

Wang, JH, Liu, XJ, and Wan, DC (2015). "Numerical Simulation of an Oblique Towed Ship by naoe-FOAM-SJTU Solver," *Proc 25th Int Offshore and Polar Eng Conf*, Hawaii, ISOPE, 432-438.

Wang, JH, and Wan, DC (2016). "Numerical Simulation of Pure Yaw Motion using Dynamic Overset Grid Technology," *Chinese J Hydrodynamics*, 31(5), 567-574.

Wang, JH, Liu, XJ, Wan, DC, and Chen, G (2016). "Numerical Prediction of KCS Self-Propulsion in Shallow Water," *Proc 25th Int Offshore and Polar Eng Conf*, Rhodes, 757-763.

Wienke, J, and Oumeraci, H (2005). "Breaking Wave Impact Force on

a Vertical and Inclined Slender Pile-theoretical and Large-scale Model Investigations," *Coast Eng*, 52(5), 435-462.

Zang, J, Taylor, PH, and Tello, M (2010). "Steep Wave and Breaking Wave Impact on Offshore Wind Turbine Foundations-Ringing Revisited," *Proc 25th Int Workshop on Water Waves and Floating Bodies*, Harbin, IWWWFB, May 9-12.

Zhao, WW, and Wan, DC (2016). "Numerical Study of 3D Flow past a Circular Cylinder at Subcritical Reynolds Number Using SST-DES and SST-URANS," *Chinese J Hydrodynamics*, 31(1), 1-8.